JURNAL POLIMESIN
Unit Penelitian dan Pengabdian Kepada Masyarakat (P2M)
Politeknik Negeri Lhokseumawe
ISSN Print: 1693-5462, ISSN Online: 2549-1199
Website: http://e-jurnal.pnl.ac.id/index.php/polimesin

Dynamic stiffness analysis of a nonlinear vibration isolation model with asymmetrical and quasi-zero stiffness characteristics

N.Y.P. Vo[1], M.K. Nguyen[2] and T.D. Le[3*]
[1]Graduation, Ho Chi Minh City University of Technology and Education – No. 1 Vo Van Ngan-Thu Duc District-Ho Chi Minh City, Viet Nam.
[2]Ho Chi Minh City University of Technology and Education- No. 1 Vo Van Ngan-Thu Duc District-Ho Chi Minh City, Viet Nam.
[3]Industrial University of Ho Chi Minh City – No. 12 Nguyen Van Bao Street-Go Vap District-Ho Chi Minh City, Viet Nam.
[*]Corresponding author E-mail: *lethanhdanh@iuh.edu.vn*

Abstract

As well known, nonlinear vibration isolation models may offer potential effectiveness for isolating low frequency vibrations. Therefore, this paper will introduce a nonlinear vibration isolation model, featuring asymmetrical and quasi-zero stiffness characteristics. Firstly, the physical model of the nonlinear vibration oscillation is shown, including a semicircular cam-roller and wedge-roller mechanism, in which cylinder adding auxiliary tank is worked as an elastic element. Secondly, its dynamic stiffness is built and numerically simulated. Based on these, the parameters which effect on dynamic stiffness of the system are identified. The analysis results confirmed that the proposed model can attain the quasi-zero stiffness by adjusting the pressure inside the cylinder of the stiffness corrected stiffness. Moreover, increasing the auxiliary tank volume will decrease the asymmetry of the stiffness curve. This study will furnish a useful insight to analyze and design a quasi-zero stiffness vibration isolator.

Keywords: Asymmetrical stiffness, Quasi-zero stiffness, Vibration Isolation

1. Introduction

In order to solve the vibration isolation problem, many researches have been carried out a lot of achievement. Each of them brings the vibration isolation field particular merits. For example, Mengnan Sun *et al.* proposed a high-static-low dynamic stiffness vibration oscillator with a novel parabolic-cam-roller negative stiffness mechanism [1]. This is an asymmetric supporting structure. Because of its asymmetry, the dynamic stiffness is not equal to zero at the equilibrium position. Although NSS does not eliminate the asymmetric in vibration, the isolation capacity of asymmetric supporting system is improved effectively. It's obvious that because of the addition of NSS, both the resonance frequency band was expanded and the vibration magnitude was reduced a lot. Besides, Xiuting Sun *et al.* [2] investigated in isolation platform with n-layer-scissor like truss structure. This nonlinear vibration isolation system can meet different stiffness and damping requirements for different types of excitation and working conditions due to the special scissor like structure, its dynamic response has inherent nonlinearities both in equivalent damping and stiffness characteristic by designing structural parameters.

Along with the previous study, in [3] Xiuting Sun *et al.* analyzed theoretically and did experiment which results in the demonstration of the advantages and versatility of the proposed system in vibration isolation because of its nonlinearity meaning that the isolation performance can be achieved much better such as not only stable equilibrium without jumping phenomenon but a very useful anti-resonance frequency band with tunable frequency band and magnitude via structure parameters. A prototype of QZS vibration isolation with cam-roller-spring which is simulated to find out the vibration isolation effectiveness at low frequency range is suggested by Jiaxi Zhou *et al.* [4]. Diego Francisco L.R. *et al.* [5] explored nonlinear stiffness elements through providing low dynamic stiffness of an isolation system electromagnets and permanent magnets to obtain nonlinear stiffness which is advantageous in improving shock isolation. Yisheng Zheng *et al.* [6] proposed an isolator which comprised of two coaxial ring permanent magnets and negative stiffness magnetic spring. This nonlinear dynamic equation of the system is able to reduce the resonance frequency and peak transmissibility of the isolator effectively which outperforms a linear isolator indeed. Another study in [7] called a

Stewart platform with high-static-low-dynamic stiffness which employed a negative stiffness spring. The composer has proved the effects of the nonlinear dynamic mode considering both geometry nonlinearity and stiffness nonlinearity on the isolation performance that the resonance frequency are reduced and the isolation region is increased. Feng Zhang *et al.* [8] suggested a new magnetic negative stiffness isolator with active-passive hybrid control based on Maxwell magnetic normal stress which can reduce the isolation initial frequency and significantly suppress the system resonance response. Besides, compact size and light weight are able to approach. Thanh Danh Le *et al.* [9] introduced a system with NSS employing slide mode control algorithm to present the nonlinear mapping between the sliding mode surface and the equivalent control effort. In new control scheme, the chattering problem was removed, the isolation effectiveness of the isolation system using negative stiffness structure was improved. The merit of this control method performed an accurate dynamic model, and the trial and error work. [10] Thanh Danh Le and Kyoung Kwan Ahn investigated a vibration isolation system with a negative stiffness structure. The nonlinear stiffness characteristic of the system is experimented which shows the wide isolation frequency band and the disappearance of the resonance phenomenon. In [11] Zhan Hu *et al.* developed an adjustable high-static-low-dynamic stiffness vibration isolator with a widely-variable stiffness. Its nonlinear dynamic feature was approximately analyzed. The results of the vibration test with the Hilbert transform the effective damping ratio will be remarkably enhanced when the AHSLD is adjusted the condition of the quasi-zero stiffness. In addition, the AHSLD isolator presents relative more hardening nonlinearity when it is adjusted to the lower stiffness condition. The quasi-zero stiffness nonlinear oscillator to achieve real-time controllable quasi-zero stiffness is proposed by Shaogang Liu *et al.* in [12]. Negative stiffness is produced by comprising of two electromagnets with MR elastomer and the experimental results confirms this isolator has a wider frequency region for vibration attenuation than the corresponding linear isolator with the active control of stiffness. The proposed QZS isolator has much higher adaptability. The effectiveness of the mode is verified. Besides, a passive nonlinear isolator by combining a negative stiffness corrector, which is formed by Euler bucked beams, to a linear spring is developed by Xiuting Liu *et al.* [13]. This model demonstrated an outstanding isolation performance which can be achieved through adjusting the initial what of the Euler beams. Recently, a QZS isolation system using negative stiffness structure for supporting different loads and improving the isolation performance based on using a multi cam-roller mechanism in low frequency range is designed by Kan Ye *et al.* [14]. Instead of using one pair of oblique spring as in [2], in [15] Fen Zhao *et al.* proposed a QZs nonlinear isolation system using two pairs of oblique springs which demonstrates a new limb-like QZS which can be adopted for suppressing low frequency vibration in engineering applications. Besides, A.D. Shaw *et al.* [16] designed and tested a simple and compact mechanical device in which a mass was suspended on a multi-modal beam structure. This system has a significant contribution is that its stiffness characteristic can not only be adjusted through adjusting two independent mechanisms but also its nonlinear stiffness is also symmetric around the equilibrium position. In [17], another type of QZS by using linear electromagnetic spring connected in parallel to a linear mass-damper-spring system was suggested by Shijin Yuan *et al.* [17] by controlling the current in the coils, the stiffness can be tuned linearly online thereby obtaining a quasi-zero stiffness via the long working stroke. A QZS vibration isolation system is usually designed for supporting a certain load. Kan Ye *et al.* [18] proposed a novel prototype QZS structure based on the cam-roller mechanism, an optimized QZS nonlinear isolator responds to different load was developed. The experimental results verify a good agreement with the theorical analysis which can be implemented into practical applications.

Isolation models with characteristic mentioned above have often used mechanical springs with fixed coefficients or magnetic spring. However, the limitation of the mechanical spring is inevitable, for instance: changing the isolated load results in the drift of the static equilibrium position compared to the desirable one. This can influence the isolation response. To surmount this issue, when the load is changed, the mechanical spring must be replaced by proper springs to remain the desirable equilibrium position. Meanwhile, the stiffness of magnetic springs can be adjusted but it is often used for low isolated load. Hence, it can cause difficulties to be practically applied.

Motivated by potential ability of the isolation method with high-static low-dynamic stiffness characteristic, the present paper will introduce an adaptive quasi-zero stiffness isolator (named AQZSI) including a load bearing mechanism connecting with a stiffness corrected mechanism in parallel. Unlike conventional QZS system, the cylinder with auxiliary tank is used as an elastic mechanism. The merit of the proposed model is that it can always remain the desirable equilibrium position regardless of the change of the isolated load through regulating the pressure. Besides, by adjusting the pressure inside cylinder, the proposed model can obtain the quasi-zero stiffness at this equilibrium position.

The paper is organized as following. The description of the model is presented in section 1, the system stiffness is established and analyzed in detail in section 2, the effects of the working parameters on the stiffness and stiffness position are considered in section 3. The conclusion is drawn in section 4.

2. Description of the proposed model

In the proposed model, Fig.1(a) shows a nonlinear isolation model, combining of an asymmetric stiffness mechanism in vertical direction in parallel with a symmetrical one. The former includes wedge (inclined angle α) 8-rollers 5-cylinder 1 with auxiliary tank 3 which produces the positive stiffness to support the load. The latter comprises semicircular cam (radius R) 7-rollers 6-cylinder 2 which generates the negative stiffness for correcting the system stiffness of the AQZSI. Fig. 1(b) presents three specific states of the AQZSI. First, at undeformed position, the forces generated by the elastic forces of the load bearing mechanism (LBM) but the stiffness corrector mechanism (SCM) are not to exist. Second, at arbitrary deformed one, the two pneumatic cylinders of two mechanisms can produce the vertical elastic forces. Third, at equilibrium one, the vertical force is only generated by the wedge mechanism. In order to ensure the contact between the surfaces of wedge and roller as well as the surface of semicircular cam and roller, the absolute pressure inside the cylinder of the load bearing and stiffness corrected mechanism must be larger than the atmospheric pressure. It is noted that during operation, all cylinders are fixed in vertical direction.

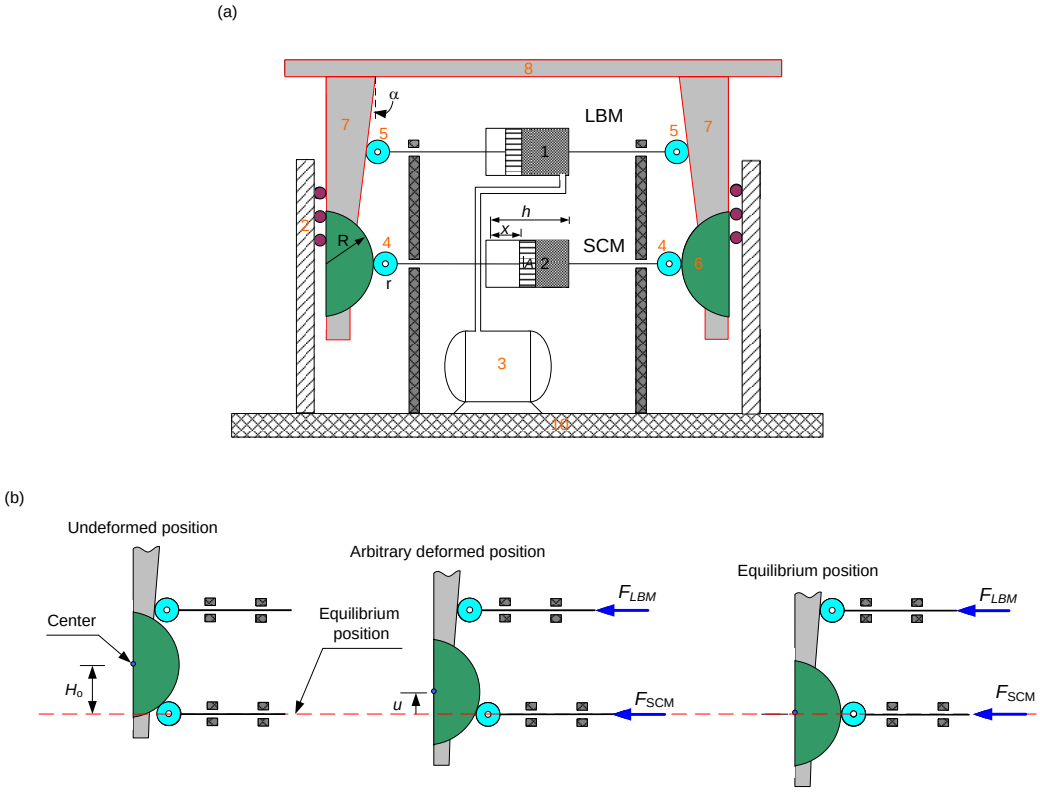

Figure. 1 (a) Schematic of the proposed asymmetric nonlinear vibration oscillator model with quasi-zero stiffness characteristic (AQZSI); (b) Scheme of distinctive positions of AQZSI

3. Dynamic stiffness analysis

By ignoring the heating exchange and friction, through the ideal gas laws, the pressure in the cylinder is calculated as below:

$$P_s = P_{so}\left(\frac{Ah + V_t}{Ah + V_t - Ax}\right)^n \qquad (1)$$

in which, V_t is the volume of the auxiliary tank; A is the area of the cylinder in m^2; P_{so} is the pressure in the cylinder at the undeformed position in Pa; h is the piston stroke in m, x is the displacement of the piston compared with the undeformed position as defined in Fig. 1, n is the ratio of specific heat capacity.

If F_s is called the result of restoring force in the vertical direction generated by the load bearing and corrected mechanism, it can be determined as

$$F_s = F_{LBM} + F_{SCM} \qquad (2)$$

where F_{LBM} and F_{SCM} are the vertical restoring forces caused by the LBM and SCM, respectively, which are compressed and generated two vertical restoring forces acting on the wedge and semicircular cam, can be derived as below

$$F_{LBM} = 2A_1\left[\begin{matrix}P_{so1}\left(\frac{A_1h_1+V_{t1}}{A_1h_1+V_{t1}-2A_1H_o\tan\alpha+2A_1u\tan\alpha}\right)^n\\ -P_{atm}\end{matrix}\right]\tan\alpha$$

$$F_{SCM} = 2A_2\left[\begin{matrix}P_{so2}\left(\frac{A_2h_2}{A_2h_2+2A_2\sqrt{(R+r)^2-H_o^2}-2A_2\sqrt{(R+r)^2-u^2}}\right)^n\\ -P_{atm}\end{matrix}\right]\frac{u}{\sqrt{(R+r)^2-u^2}} \qquad (3)$$

in which α is the angle of the table leg, R is the radius of the semicircular cam, r is the radius of rollers, u is the displacement of the cam compared with the equilibrium position as shown in Fig. 1b, P_{atm} is the ambient pressure in Pa; subscripts 1 and 2 are denoted the pneumatic cylinders 1 and 2, respectively.

Dimensionless static dynamic stiffness of the system is derived by taking derivation of Eq. (2):

$$\hat{K}_s = 4n\frac{\hat{V}_{d1}^n\hat{V}_{e01}^n\tan^2\alpha}{\left(\hat{V}_{e01}-2\hat{H}_o\tan\alpha+2\hat{u}\tan\alpha\right)^{n+1}} + \frac{2\hat{A}}{\sqrt{1-\hat{u}^2}}\left[\hat{P}_{atm}-\mu\hat{V}_{d2}^n\left(\frac{\hat{V}_{e02}}{\hat{V}_{e02}+2\hat{A}\sqrt{1-\hat{H}_o^2}-2\hat{A}\sqrt{1-\hat{u}^2}}\right)^n\right]\left(\frac{1}{1-\hat{u}^2}\right) + \frac{\hat{u}^2}{1-\hat{u}^2}\frac{4n\mu\hat{A}^2\hat{V}_{d2}^n\hat{V}_{e02}^n}{\left(\hat{V}_{e02}+2\hat{A}\sqrt{1-\hat{H}_o^2}-2\hat{A}\sqrt{1-\hat{u}^2}\right)^{n+1}} \qquad (4)$$

where $\hat{K}_S = \frac{K_S b}{A_1P_{d1}}$ $\hat{A} = \frac{A_2}{A_1}$; $\hat{H}_o = \frac{H_o}{R+r}$; $\hat{P}_{atm} = \frac{P_{atm}}{P_{d_1}}$; $\hat{u} = \frac{u}{R+r}$;

$\hat{V}_{e01} = \frac{A_1h_1+V_{t1}}{A_1(R+r)}$; $\hat{V}_{e02} = \frac{A_2h_2}{A_1(R+r)}$; $\hat{V}_{d1} = \frac{V_{d1}}{V_{e01}}$;

$\hat{V}_{d2} = \frac{V_{d2}}{V_{e02}}$; $\hat{F}_{LBM} = \frac{F_{LBM}}{A_1P_{d1}}$; $\mu = \frac{P_{d2}}{P_{d1}}$. (5)

It is necessary to express the exact restoring force around the wanted equilibrium position through expanding the Taylor series following:

$$F_{eq} = F_o + a_1u + a_2u^2 + a_3u^3 + a_4u^4 + a_5u^5 + \mathrm{O}(u^6) \qquad (6)$$

herein,

$$F_o = 2A_1\left[\begin{matrix}P_{so1}\left(\frac{A_1h_1+V_{t1}}{A_1h_1+V_{t1}-2A_1H_o\tan\alpha}\right)^n\\ -P_{atm}\end{matrix}\right]\tan\alpha \qquad (7)$$

$$a_n = \frac{1}{n}\left(\frac{dF_{LBM}{}^n}{du^n}+\frac{dF_{SCM}{}^n}{du^n}\right)\Bigg|_{u=0} \quad n = 1,2,3,4,5 \qquad (8)$$

In order to make sure that the restoring force derived from expanding Taylor series is in good agreement with the mathematical elastic force in Eq. (2), a numerical simulation is shown in Fig. 2a. In this figure, the former is drawn by the dot line, the latter is presented by the solid line. It is clearly that around the equilibrium position, the error between them is an extremely small value which is illustrated in Fig. 2b. Hence, this 5th - order polynomial is suitably applied to analyze the system dynamic stiffness characteristics.

(a)

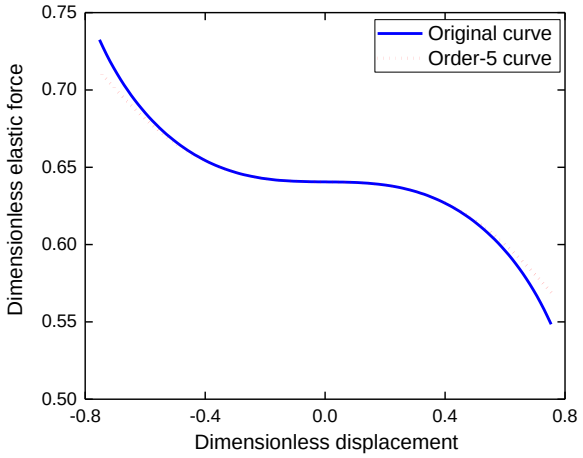

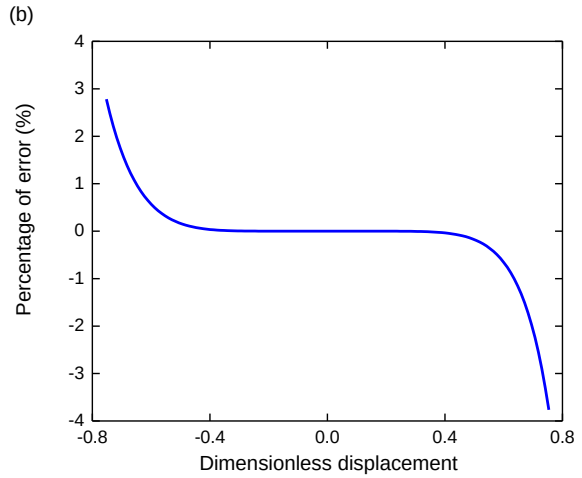

Figure 2. (a) Comparison between the elastic forces curve of the exact (solid line) and Taylor approximated force (dot line); (b) The error percentage between these solutions.

4. Results and Discussion.

4.1. *The working condition of the two mentioned mechanisms*

In order to be able to support the load in desired working region, the initial absolute pressure P_{so1} of LBM must be larger than one. The requirement is that $|u| \le H_o$. It means that

$$\frac{2A_1H_o\tan\alpha}{A_1h_1+V_{t1}} < 1-\frac{1}{\left(P_{ep1}\right)^{1/n}} \qquad (8)$$

At the equilibrium position, the weight of the isolated load is calculated as below:

$$M = \frac{P_{so1}A_1}{g}\left(\frac{A_1h_1+V_t}{A_1h_1+V_t-2A_1H_o\tan\alpha}\right)^n \qquad (9)$$

Substituting Eq. (9) into Eq. (8), we obtain:

$$\frac{2A_1H_o\tan\alpha}{A_1h_1+V_{t1}} < 1-\left(\frac{A_1}{Mg}\right)^{1/n} \qquad (10)$$

In order to investigate which factors affect directly on the asymmetry and quasi-zero stiffness characteristics, the two working parameters including auxiliary tank volume and pressure ratio are analyzed numerically simulated.

For instance, H_o=73.5mm and A_1=0.0095m^2, through Eqs. (9), the relationship between the weight of the isolated load and the initial volume for which the pressure in the cylinder 1 is always higher than one as shown in Fig. 2. It can be seen that either increasing the initial pressure or reducing the tank volume will result in an increase in the isolated load. However, the effect of these parameters on the isolated load is different. Specifically, the isolated load is almost increased gradually according to the growth of the initial pressure as observed in Fig.2(b) created by a cutting section V_t=0.01m^3 meanwhile the figure 2(c) cut by a section at P_{so1}=2 bar indicated that the isolated mass can be varied remarkably as there is a change of the tank volume in the region less than 0.05m^3.

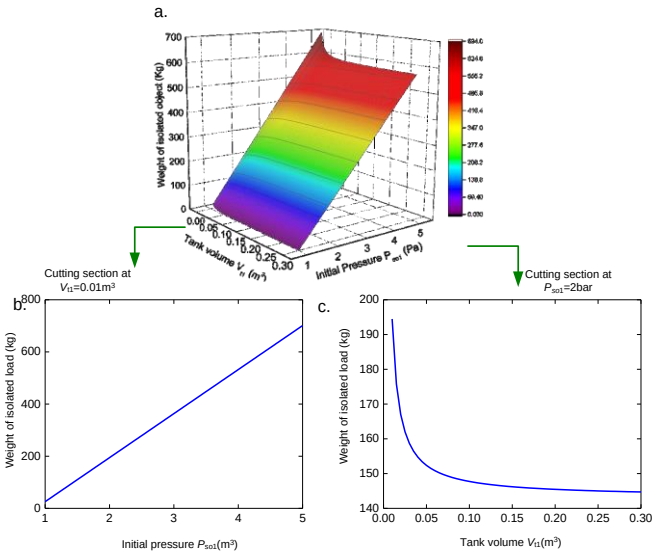

Figure 3. (a) The dependence of the isolated load on the tank volume and initial pressure of the cylinder 1 with H_o =73.5mm; and A_1 = 0,0095m^2. (b) Relation of the isolated mass and the initial pressure P_{so1} for V_{t1}=0.01m^3, (c) Relation of the isolated mass and tank volume V_{t1} for P_{so1}=2 bar

In the same way, the stiffness corrected mechanism only takes up its duty when its absolute pressure in the cylinder larger than 1 bar. To ensure this requirement, the working region of the SCM is predicted as follow:

$$|u| \le u_{L\_SCM} = \sqrt{(R+r)^2-\left(\frac{V_{a2}+2A_2\sqrt{(r+R)^2-H_o^2}-V_{e2}\left(\frac{\mu Pe_1}{P_{atm}}\right)^{1/n}}{2A_2}\right)^2} \qquad (11)$$

4.2 Numerical simulation of the dynamic stiffness

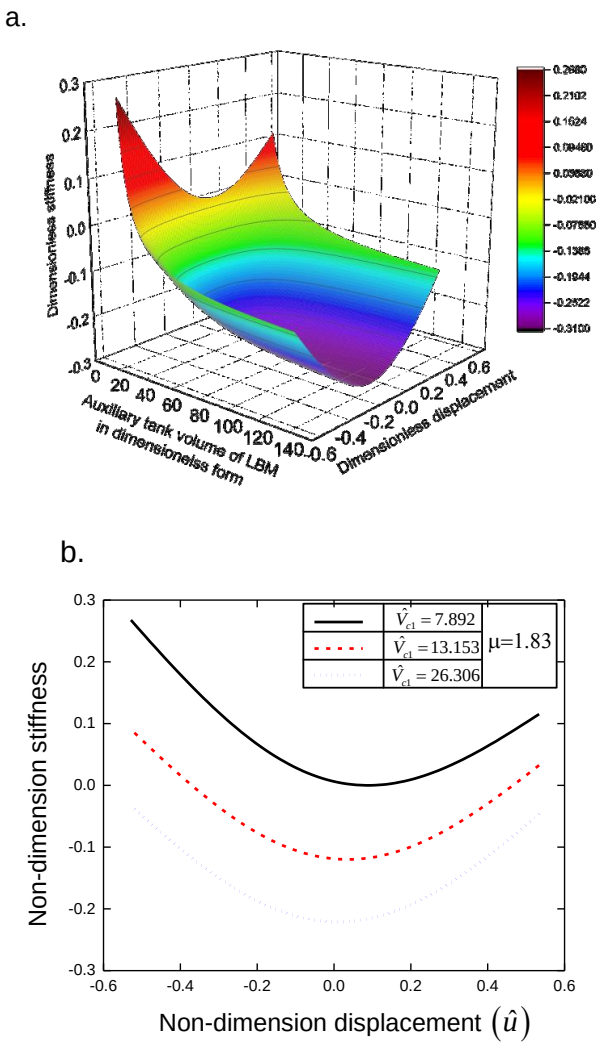

Figure 4. The vertical stiffness surface in the space $\left(\hat{V}_{t1}, \hat{u}_h, \hat{K}_s\right)$

In Fig. 4a, the dynamic stiffness surface in the space with three parameters $\hat{V}_{t1}, \hat{u}_h, \hat{K}_s$, with the pressure ratio is 1.83 illustrated the effects of the auxiliary tank volume of LBM on the stiffness system. It can be seen that the dynamic stiffness of the AQZSI is an asymmetrical concave parabola. Simultaneously, both the stiffness value and its asymmetry will be reduced as the volume in the auxiliary tank is increased. As shown in Fig. 4b line types are denoted in the right-corner panel. As the dimensionless volume of the auxiliary tank increases to the value of 23.306 m^3, the position at which the stiffness obtains the minimum value is close to the equilibrium position, indicating that the asymmetric level of the AQZSI is remarkably lessened. Particularly, in Fig. 5 which shows the impact of the auxiliary tank volume V_{t1} on the minimum stiffness position, showing that the position obtaining the minimum stiffness is toward to the equilibrium position as the tank volume of the load bearing mechanism is increased.

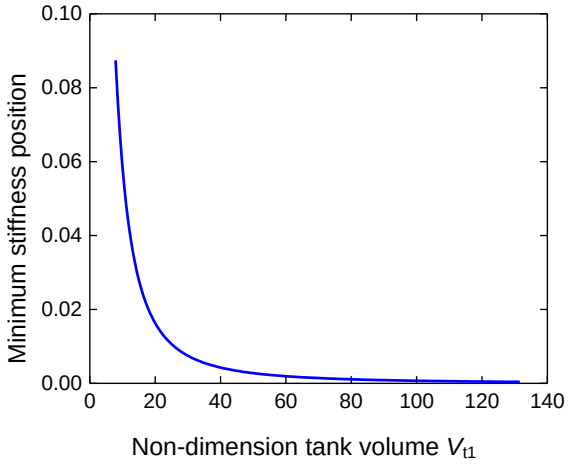

Figure 5. The influence of auxiliary tank volume $\hat{V}_{t1}$ on the minimum stiffness position.

Fig. 6a points up the relationship between the pressure ratio μ and the auxiliary tank volume of LBM for which the pressure in cylinder of the SCM will be predicted so that the stiffness of proposed system equals to zero. It's obviously that the form of the pressure ratio curve is an asymmetrical parabola. In addition, it also revealed that increasing the dimensionless volume of the tank leads to a reduction in the pressure ratio and the asymmetric of the pressure ratio curve. Indeed, as shown in Fig. 6b, if $\hat{V}_{t1} = 7.982$, the minimum value of μ for which the system can offer the zero stiffness is 1.834 (at point D) and the position of this point is determined at $\hat{u} = 0.1$ but if the dimensionless value of V_{t1} is increased to 34.198, the minimum value of μ is reduced to 0.905 corresponding to point A ($\hat{u} = 0.01$).

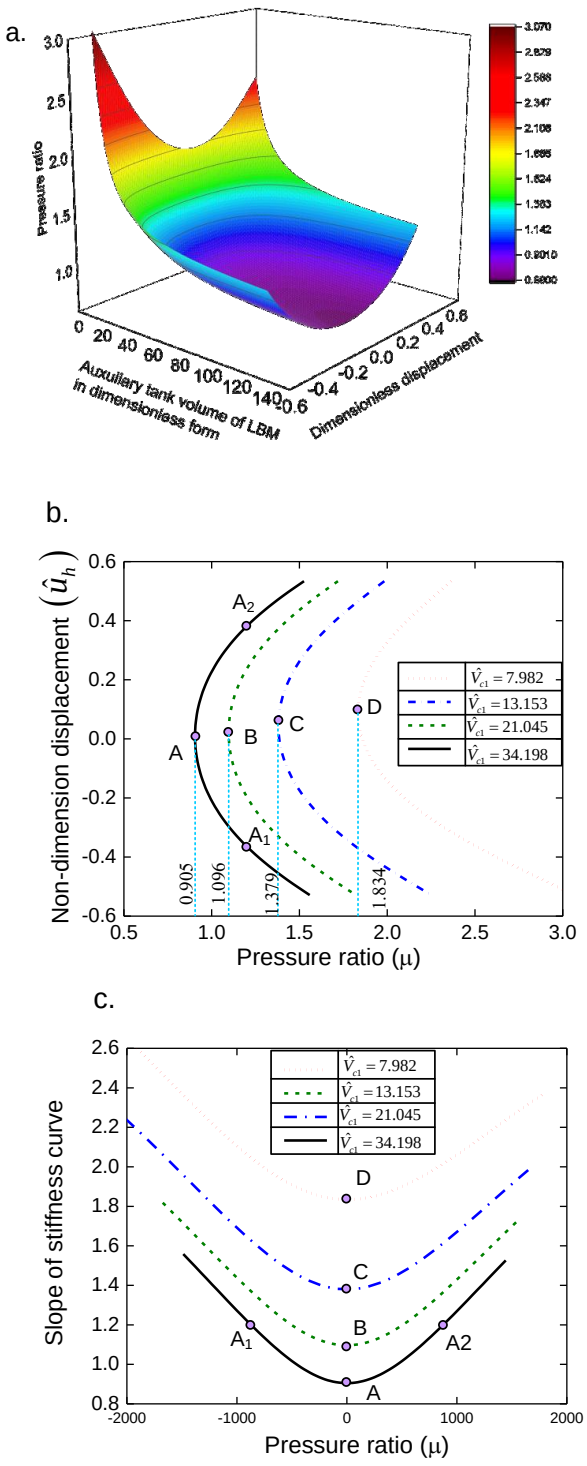

Figure 6. (a). The quasi-zero stiffness surface in the space $(\hat{V}_{t1}, \hat{u}_h, \mu)$; (b). The pressure ratio curve for various values of the $\hat{V}_{t1}$; (c) The slope of the dynamic stiffness versus the pressure ratio.

Furthermore, the slope of the stiffness curve is equal to zero at external points (A, B, C, D) of the pressure ratio curves or nonzero at points (for example A_1 or A_2) moving away from extreme as shown in Fig. 7b, which infers that with values of μ=0.905, 1.096, 1.379 and 1.834 corresponding to at points A, B, C, D, respectively, the AQZSI will achieve minimum stiffness and its value is equal to zero. As seen in Fig. 7a. But if the value of μ is different from these values the minimum stiffness of the system can be positive or negative. For instance, $\hat{V}_{t1}=34.198,$ the minimum dynamic stiffness will be positive for values of μ<0.905 and negative for μ>0.905 as shown in Fig. 7b. This is evident, if μ=1.2, the system will offer two positions A_1 and A_2 marked by the filled circles in Fig. 7b at which the dynamic stiffness is equal to zero. However, the slope of the stiffness curve at these points is nonzero as shown in Fig. 7b. Therefore, the stiffness at points A_1 and A_2 cannot be the minimum value.

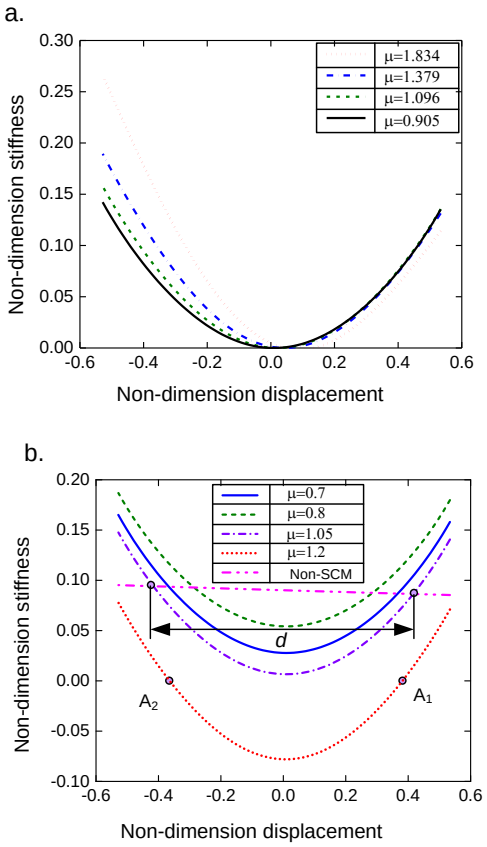

Figure 7. Stiffness curve for different values of μ given in the panel of the figure, the same other parameters as in Fig. 5.(a) Quasi-zero stiffness at the position $(\hat{u}=0.008, 0.021, 0.046, 0.083)$, (b) Arbitrary stiffness.

These simulated results reveal that the stiffness of the proposed model is adjusted by regulating the pressure inside the cylinder of the SCM. Meanwhile, the proposed model can remain the desirable equilibrium position as there is a change in the isolated load through the regulating of the pressure inside the cylinder of the LBM. Additionally, increasing the auxiliary tank volume will improve the symmetry of the stiffness curve. With proper values of these parameters, the AQZSI can obtain the quasi-zero stiffness close to the equilibrium position.

5. Conclusions.

This paper has presented the design, dynamic stiffness analysis of an asymmetric quasi-zero-stiffness vibration isolator, in which the cylinder of the LBM added with the auxiliary tank is used to reduce the asymmetric of the stiffness curve around the equilibrium position meanwhile the proposed system can offer the quasi-zero stiffness through the SCM. Firstly, the dynamic stiffness of the proposed model was established, the numerical calculation of which was then realized. The analysis result confirmed that increasing the auxiliary tank volume will decrease the asymmetric of the stiffness curve. It means that the minimum stiffness position is towards the equilibrium position. Besides, instead of either replacing the elastic structures or correcting the configuration parameters, this model only adjusts the pressure ratio easily to achieve the desirable stiffness, even it is able to obtain quasi-zero stiffness. Furthermore, this work had determined the working conditions for which, the all rollers always contact with the surface of the wedge and semicircular cam.

Acknowledgement: This work belongs to the project grant No: T2020-05NCS funded by Ho Chi Minh City University of Technology and Education, Vietnam.

Nomenclature

AQZSI : Adaptive quasi-zero stiffness isolator
AHSLD : Adjustable high-static-low-dynamic
LBM : Load bearing mechanism
NSS : Negative stiffness structure
QZS : Quasi-zero stiffness
SCM : Stiffness corrected mechanism

References.

[1] Mengnan Sun, G. S., "Effect of negative stiffness mechanism in a vibration isolator with asymmetric and high-static-low-dynamic stiffness", *Mechanical Systems and Signal Processing*, 388-407, 2019.

[2] Xiuting Sun, X. J., "Vibration isolation via a scissor-like structured platform", *Journal of Sound and Vibration*, 2404-2420, 2014.

[3] Xiuting Sun, X. J., "A nonlinear vibration isolator achieving high-static-low-dynamic-stiffness and tunable anti-resonance frequency band", *Mechanical Systems and Signal Processing*, 04-011, 2016.

[4] Jiaxi Zhou, X. W., "Nonlinear dynamic characteristics of a quasi-zero stiffness vibration isolator with cam-roller-spring mechanisms", *Journal of Sound and Vibration*, 53-692, 015.

[5] Diego Francisco L.R., N. S., "An experimental nonlinear low dynamic stiffness device for shock isolation", *Journal of Sound and Vibration*, 1-13, 2015.

[6] Yisheng Zheng, X. Z., "Design and experiment of a high-static-low-dynamic stiffness isolator using a negative stiffness magnetic spring", *Journal of Sound and Vibration*, 31-52, 2016.

[7] Yisheng Zheng, Q. P.," A Stewart isolator with high-static-low- dynamic stiffness struts based on negative stiffness magnetic springs", *Journal of Sound and Vibration*, 390-408, 2018.

[8] Feng Zhang, S. S., "Active-passive hybrid vibration isolation with magnetic negative stiffness isolator based on Maxwell normal stress", *Mechanical Systems and Signal Processing*, 244-263, 2019.

[9] Thanh Danh Le, M. T., "Improvement of Vibration isolation performance of isolation system using negative stiffness structure", *Vol.21*, p. 1561, 2016.

[10] Thanh Danh Le, K. K. Ahn, "Experimental investigation of a vibration isolation system using negative stiffness structure", *International Journal of Mechanical Sciences*, 99-112, 2013.

[11] Zhan Hu, X. W., "Theoretical analysis and experimental identification of a vibration isolator with widely-variable stiffness" *Journal of Vibration and Acoustics*, 1-21, 2018.

[12] Shaogang Liu, L. F., "A real-time controllable electromagnetic vibration isolator base on magneto-rheological elastomer with quasi zero stiffness characteristics, *Journal of Smart Material and Structures*, 1-28, 2019.

[13] Xingtian Liu, X. H., "On the characteristics of a quasi-zero stiffness isolator using Euler buckled beam as negative stiffness corrector", *Journal of Sound and Vibration*, 3359-3376, 2013.

[14] Kan Ye, J. J., "Design of a quasi-zero stiffness isolation system for supporting different loads", *Journal of Sound and Vibration*, 21, 2020.

[15] Feng Zhao, J.C. J., K. Y., Q. L., "Increase of quasi-zero stiffness region using two pairs of oblique Springs", *Mechanical Systems and Signal Processing*, 144, 106975, 2020.

[16] A.D. Shaw, G. G., P.J.P. G., B. T., M.J. B., "Design and test of a adjustable quasi-zero stiffness device and its use to suspend masses on a multi-modal structure", *Mechanical Systems and Signal Processing* 152,107354, 2021.

[17] Shujin Yuan, Y. S., J Z., K. M., M. Wang, H. Pu., Y. P., J. L., S. X., "A tunable quasi-zero stiffness isolator based on a linear electromagnetic spring", *Journal of Sound and Vibration* 482, 115449, 2020.

[18] Kan Ye, J.C. J., T. B., "Design of a quasi-zero stiffness isolation system for supporting different loads", *Journal of Sound and Vibration*, 471, 115198, 2020.